

Thermodynamics and non-isothermal kinetics of solid-state decomposition of poly-2-dimethyl amino ethyl methacrylate NFGs derived from supercritical CO₂

P. Joshi^{1*}, M. Pandey^{3*}, M. Aziz², I. Joshi², D. Palariya², M. Pandey², S. Mehtab², M.G.H. Zaidi²

¹Department of Chemistry, School of Allied Sciences, Dev Bhoomi Uttarakhand University, Naugaon 248007, India

²Department of Chemistry, College of Basic Sciences and Humanities, G.B. Pant University of Agriculture and Technology, Pantnagar, U.S Nagar 263145, Uttarakhand, India

³Department of Chemistry, School of Science, IFTM University, Moradabad-244102, Uttar Pradesh, India

Received: March 20, 2023; Revised April 20, 2023

Nanoferrogels (NFGs) are potentially valuable materials for various agricultural and biomedical applications, where thermal resistance is crucial for effectiveness and safety. In this study, the thermodynamic and non-isothermal kinetic properties of the solid-state decomposition of supercritically synthesized poly-2-dimethyl amino ethyl methacrylate (PDMAEMA) and its NFG were investigated. NFGs were prepared by incorporating ferrite nanoparticles (FNPs) of size ~ 10.5 nm through a chemical method. Kinetic and thermodynamic characteristics of NFGs were demonstrated through thermal analysis. By comparing NFGs non-isothermal kinetic, thermal and thermodynamic data with that of FNP and PDMAEMA, this study aimed to gain insight into the unique properties of NFG. PDMAEMA have shown three-step decomposition, leaving a char residue of 25.7%. NFG has shown four-step decomposition, leaving 9.1% weight residue which suggests that NFG has better thermal stability and resistance to decomposition than PDMAEMA. Coats-Redfern (CR) and Horowitz-Metzger (HM) methods were used to evaluate the thermodynamics and kinetics of degradation and the thermodynamic stability of materials. HM method yielded higher values of activation energy (E_a) and pre-exponential factor (A) compared to the CR method. A slight variation was observed in ΔS and ΔH values obtained from the HM and CR methods during the evaluation process.

Keywords: Nanoferrogel, non-isothermal kinetics, supercritical, acrylate

INTRODUCTION

Ferrogels are a type of hydrogels that contain magnetic particles, such as iron oxide nanoparticles, dispersed throughout hydrophilic monomers, e.g., acrylic acid or acrylamide [1, 2]. Ferrite nanoparticles (FNPs) are incorporated into the hydrogel network either by embedding them within the polymer chains or by coating them onto the surface of the polymer chains [3, 4]. Ferrogels have the potential to revolutionize agriculture by improving soil remediation, nutrient delivery, plant growth, and crop monitoring [5, 6].

In agriculture, ferrogels can be used to remediate contaminated soils by absorbing and immobilizing heavy metals, pesticides, and other pollutants [7-9]. These smart materials can be loaded with nutrients and fertilizers and used to deliver them directly to plant roots [10]. The magnetic particles in the ferrogel can be manipulated with an external magnetic field to guide the gel to the desired location, resulting in more efficient nutrient uptake and reduced fertilizer waste [11-13].

Ferrogels are synthesized using sol-gel synthesis, co-precipitation, electrospinning and supercritical synthesis [14-18]. Supercritical methods are used to

tune the porosity and morphology of the ferrogel, which can affect its magnetic and mechanical properties [19, 20-22]. Thermal stability of ferrogels is essential in agriculture because it allows for the controlled release of fertilizers and pesticides over an extended period of time, which can increase their efficacy and reduce the negative impact on the environment [23, 24]. The thermal stability of ferrogels ensures that the encapsulated compounds remain intact and do not degrade or evaporate due to high temperatures or UV exposure, which can reduce their efficacy [25]. When the soil temperature reaches a certain threshold, the ferrogels can undergo a phase transition and release the encapsulated compounds into the soil. By controlling the release of these compounds, ferrogels can reduce the amount of runoff and leaching that occurs, which can lead to water pollution and soil degradation [26, 27].

Common methods for examining the thermal characteristics of materials include differential thermogravimetry (DTG), thermogravimetry (TG), and differential thermal analysis (DTA) [28-31]. Coats-Redfern (commonly known as CR) and Horowitz - Metzger (commonly known as HM) techniques have been used to analyze thermal data

* To whom all correspondence should be sent:

E-mail: pragatijoshi91@gmail.com
minakshipandey2912@gmail.com

in order to calculate the activation energy (E_a) and pre-exponential factor (A) for the thermal degradation of a material [32, 33]. The slope of the straight line and its intercept may be used to determine changes in entropy (ΔS), enthalpy (ΔH), and free energy (ΔG) from the presented data. Generally speaking, the HM and CR approaches are helpful for examining the thermal behavior of materials, including ferrogels, and can offer relevant data on their thermal stability and breakdown kinetics [13, 34].

EXPERIMENTAL

Materials

The compounds AIBN, MBA and simazine (99%) were procured from MS HiMedia Chemicals in India whereas 2-dimethyl amino ethyl methacrylate (DMAEMA) was purchased from Poly Science in the United States. The remaining substances — chemicals, solvents, and CO₂ (with 99.5% purity) — were purchased locally and were used without additional purification.

Preparation of NFG in SCC

A reactor under high-pressure with a 100 mL stainless steel vessel and temperature control was utilized to synthesize NFG. DMAEMA, AIBN, MBA and FNP with concentrations of 6.30×10^{-3} mol/dL, 1.50×10^{-3} mol/dL, 9.80×10^{-4} mol/dL and 0.03 g, w/w 3% respectively, were all added to the reactor. After this the reaction mixture was cooled down to 10°C over the course of ten minutes, CO₂ was added to raise the pressure to 1200 psi at $90 \pm 1^\circ\text{C}$. After allowing the reaction mixture to heat for 6 hours, the reactor vessel's temperature was brought down to $25 \pm 1^\circ\text{C}$, and the contents were depressurized at a rate of 1 mL/min to produce NFG. In SCC, PDMAEMA was produced by polymerizing DMAEMA in the absence of FNP under the same reaction conditions.

CHARACTERIZATION

Utilizing alumina as a reference, the thermo-oxidative stability of the samples was examined utilizing simultaneous TG-DTG-DTA over EXSTAR TG/DTA 6300 at a heating rate of 10 °C/min in air (200 ml/min). TG data were interpreted for evaluation of moisture content, char yield, % weight residue of samples along with kinetic and thermodynamic factors.

Interpretation of TG

TG data of PDMAEMA, NFG were evaluated for their weight loss (%) with reference to temperature, decomposition stages involved and kinetic parameters through a series of calculation-based methods such as CR and HM methods.

Plotting the double logarithm of the reciprocal of the weight fraction of the reactant component against temperature is what is entailed in the HM method. The following equation (Eq. (1)) serves as a description of the HM approximation expression:

$$\log\left(\log\left(\frac{w_0}{w}\right)\right) = \frac{E_a \theta}{2.303RT_s^2} \quad (1)$$

with w_0 : the initial weight; w : the weight at temperature T; $w/w_0 = 0.368$ for 1st order reaction and T_s : the experimental reference temperature such that $T - T_s = \theta$.

For the CR method, the equation is as follows:

$$\log_{10}\left[-\frac{\log_{10}(1-\alpha)}{T^2}\right] = \left[\log_{10}\left(\frac{AR}{aE_a}\right)\left\{1 - \frac{2RT}{E_a}\right\}\right] - \frac{E_a}{2.303RT} \quad (2)$$

where: T is the temperature in Kelvin, α is the fraction of the original sample left at temperature T and R is the universal gas constant with a value of $8.314 \text{ JK}^{-1}\text{mol}^{-1}$ in SI units. CR method implies a plot of $\log_{10}[-\log_{10}(1-\alpha)/T^2]$ vs T^{-1} for determining the energy of activation which is calculated by the straight line's slope obtained from $-(E_a/2.303R)$.

RESULTS AND DISCUSSION

Thermal stability

The TG-DTA-DTG analysis results of PDMAEMA and NFG are summarized in Table 1. PDMAEMA showed 1st decomposition step with TGo at 200°C, leaving a Wr of 87.0%. The DTG showed a 2nd decomposition step at 300°C with a Wr of 69.4%. A 3rd decomposition step occurred at 400°C, leaving a Wr of 44.1%. The TG endset of PDMAEMA showed up at 500°C, leaving a char residue of 25.7%. NFG showed 1st decomposition step with TGo at 200°C, leaving a Wr of 89.0%. A 2nd decomposition step occurred at 300°C with a Wr of 66.4%. A 3rd decomposition step occurred at 400°C, leaving a Wr of 39.3%, and a 4th decomposition step occurred at 485°C, leaving a Wr of 9.1%.

Table 1. Thermal data of PDMAEMA and respective NFG

Polymers	TG ^A		DTA ^B		-ΔH ^C	DTG ^D	
	TGo	TGe					
PDMAEMA	87.00 [200]	25.70 [500]	-6.40 [76]	67.10 [532]	0.17	20.10 [71]	26.10 [539]
NFG	89.00 [200]	9.10 [485]	190.50 [476]		-2.79	16.90 [63]	58.30 [471]

^A: TGo= %Wr at TG onset (°C), TGe= %Wr at TG endset (°C)

^B: DTA signal (Peak temperature, °C)

^C: Heat of fusion (J/g)

^D: R= Rate of degradation, kJ/g. (Peak temperature, °C)

Table 2. Kinetic and thermodynamic parameters of PDMAEMA and NFG evaluated from HM and CR methods

	T(K)	n	Method	E _a ^A	A ^B	-ΔS ^C	-ΔH ^D	ΔG ^E	R ²
PDMAEMA			CR	8.3	0.04	0.34	2.68	2.18	0.99396
	651	0	HM	25	0.07	0.40	19.3	2.02	0.99490
			CR	13	0.02	0.34	7.38	2.13	0.99516
		1	HM	32	0.03	0.37	26.3	2.14	0.99511
			CR	28	0.47	0.33	22.3	1.92	0.99712
		2	HM	38	1.20	0.36	32.3	2.02	0.99676
NFG			CR	28	0.47	0.71	22.3	4.39	0.99894
		3	HM	42	6.18	0.28	36.3	1.45	0.99728
	612	0	CR	8.7	0.04	0.34	2.51	2.05	0.99024
			HM	18	0.24	0.32	11.8	1.84	0.99705
		1	CR	20	0.01	0.34	13.8	1.94	0.99486
			HM	45	7.70	0.30	38.8	1.44	0.99861
		2	CR	42	0.10	0.33	35.8	1.66	0.99180
			HM	75	10.2	0.28	68.8	1.02	0.99736
		3	CR	67	32	0.33	58.8	1.43	0.99169
			HM	77	38	0.27	70.8	0.94	0.99731

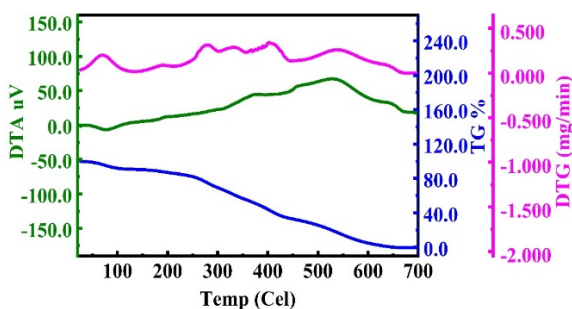


Fig. 1a. Graph simultaneously showing TG-DTA-DTG of PDMAEMA

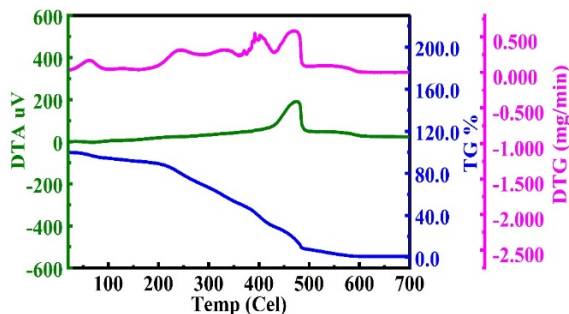


Fig. 1b. Graph simultaneously showing TG-DTA-DTG of NFG

Kinetic analysis

Utilizing alumina as a reference, the thermo-oxidative stability of the prepared samples was examined by simultaneous TG-DTG-DTA over EXSTAR TG/DTA 6300. The examination was done at a heating rate of 10°C/min in air. TG data was interpreted for evaluation of moisture content, char yield, % weight residue of samples along with kinetic and thermodynamic parameters. CR method was applied to calculate the thermodynamic and non-isothermal kinetic parameters from the TG data. CR method implies a plot between $\log_{10} [-\log_{10}(1-\alpha)/T^2]$ and T^{-1} in order to determine activation energy calculated by the straight line's slope obtained from $(E_a/2.303R)$

The kinetic and thermodynamic parameters that were deduced from the TG data using the CR and HM methods for $n = 0$ to 3 are summarized in Table 2. Table 2 also shows the regression coefficients (R^2) evaluated from the plots. The values of R^2 being approximately equal reveal their linearity. FNPs, PDMAEMA and respective NFG, reveal higher values for E_a and A evaluated from HM method over CR method. For PDMAEMA (Fig. 2a), and respective NFG HM (CR) methods reveal E_a ranging

from 25 to 42 (8.3-28) and from 23 to 76 (9.8 to 55), respectively (Figs. 2a-2d). The very high values of activation energy (E_a) in Table 2 reveal enhanced thermal stability of hydrogels and related NFG. The values of the frequency factor for CR (HM) were ranging 0.03-6.18 (0.02-0.47) and 0.24-38 (0.04-32), respectively (Figs. 2a-2d). The methods reveal ($-\Delta S$) ranging 0.40-0.28 (0.71-0.33) and 0.34-0.33 (0.33-0.32), respectively (Figs. 2a-2d). The ΔG of PDMAEMA evaluated by HM (CR) methods was found ranging 1.45 to 2.14 (1.92-4.39), respectively (Fig. 2). Under similar conditions for NFG, HM (CR) method revealed ΔG ranging 0.94 - 1.84 (1.43 to 2.05) [35].

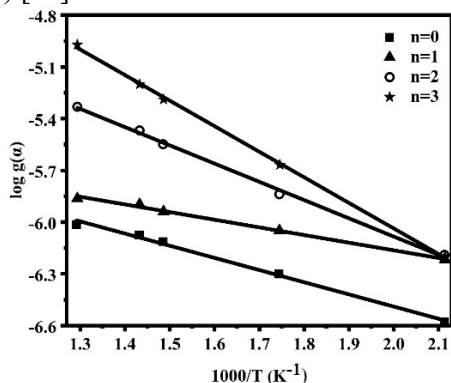


Fig. 2a. CR plots of PDMAEMA

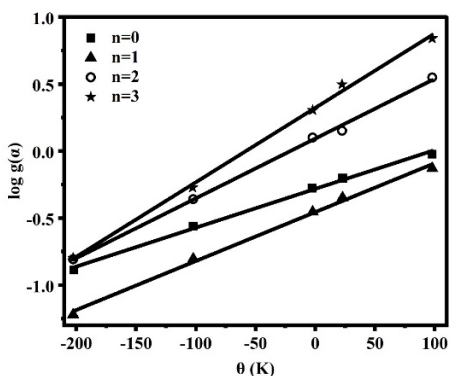


Fig. 2b. HM plots of PDMAEMA

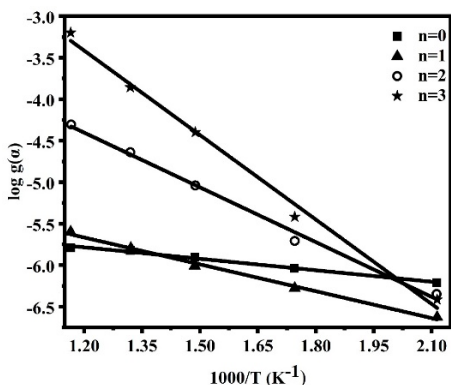


Fig. 2c. CR plots of NFG

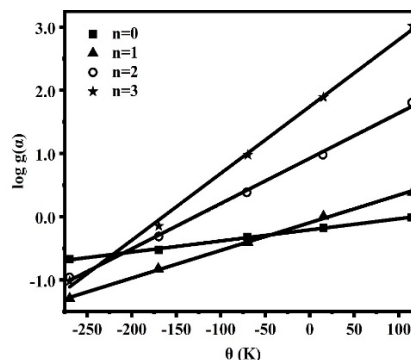


Fig. 2d. HM plots of NFG

CONCLUSIONS

Supercritical carbon dioxide was used to synthesize poly-2-dimethyl amino ethyl methacrylate (PDMAEMA) and related nanoferrogels (NFG). Coats-Redfern, commonly known as the CR method and Horowitz-Metzger, commonly known as the HM method, were employed to investigate their kinetics and the thermodynamics of solid-state decomposition at various levels ($n = 0, 1, 2,$ and 3). Both methods are widely used for the analysis of chemical reactions and are applicable to a wide range of systems. The non-isothermal kinetics were examined by plotting the $\log(\alpha)$ functions, which were calculated from TG data, against the decomposition time from thermograms. The values of E_a (activation energy) and A (frequency factor) revealed that the ferrite nanoparticles follow first-order kinetics, while PDMAEMA and NFG follow third-order kinetics. The HM method reveals higher values for E_a and A , but DS and DH showed identical results. The overall results obtained from CR and HM methods can be used to compare the reaction kinetics and thermodynamics of different systems, and to optimize reaction conditions for desired outcomes.

Acknowledgement: Authors are grateful to Defence Research Development Organization, Ministry of Defence, India, for financial support vide grant No CFEES/TCP/EnSG/CARS/Pantnagar/MOFW/20/20 18 for development of experimental facilities at Pantnagar.

REFERENCES

1. C. Boztepe, M. Daskin, A. Erdogan, *React. Funct. Polym.*, **173**, 105219 (2022).
2. A. P. Safronov, B. J. Stadler, J. Um, M. R. Zamani Kouhpanji, J. Alonso Masa, A. G. Galyas, G. V. Kurlyandskaya, *Materials*, **12**, 2582 (2019).
3. S. Awasthi, *JOM*, **73**, 2440(2021).
4. R. Messing, N. Frickel, L. Belkoura, R. Strey, H. Rahn, S. Odenbach, A. M. Schmidt, *Macromolecules*, **44**, 2990 (2011).

5. B. Narjary, P. Aggarwal, S. Kumar, M. D. Meena, ICAR (2013).
6. M. R. Guilherme, F. A. Aouada, A. R. Fajardo, A. F. Martins, A. T. Paulino, M. F. Davi, A. F. Rubira, E. C. Muniz, *Eur. Polym. J.*, **72**, 365 (2015).
7. J. Y. Lim, S. S. Goh, S. S. Liow, K. Xue, X. J. Loh, *J. Mater. Chem. A*, **7**, 18759 (2019).
8. L. M. Sanchez, D. G. Actis, J. S. Gonzalez, P. M. Zélis, V. A. Alvarez, *J. Nanopart. Res.*, **21**, 1 (2019).
9. O. V. Kharissova, H. R. Dias, B. I. Kharisov, *RSC Adv.*, **5**, 6695 (2015).
10. D. Fouad, Y. Bachra, G. Ayoub, A. Ouaket, A. Bennamara, N. Knouzi, M. Berrada, in: Chitin and chitosan-physicochemical properties and industrial applications, IntechOpen, 2020.
11. S. Agila, J. Poornima, in: 15th International Conference on Nanotechnology (IEEE-NANOIEEE), 2015, p 1058.
12. R. D. Silva, L. T. de Carvalho, R. M. de Moraes, S. D. F. Medeiros, T. M. Lacerda, *Macromol. Chem. Phys.*, **223**, 2100501 (2022).
13. P. Joshi, G. Bisht, S. Mehtab, M. G. H. Zaidi, *Mater. Today Chem.*, **62**, 6814 (2022).
14. E. I. Wisotzki, D. Eberbeck, H. Kratz, S. G. Mayr, *Soft Matter*, **12**, 3908 (2016).
15. R. Hernández, V. Zamora-Mora, M. Sibaja-Ballesteros, J. Vega-Baudrit, D. López, C. Mijangos, *J. Colloid Interface Sci.*, **339**, 53(2009).
16. N. A. Elkasabgy, A. A. Mahmoud, *AAPS PharmSciTech*, **20**, 256 (2019).
17. P. Joshi, S. Mehtab, M. G. H. Zaidi, *Bull. Chem. Soc. Jpn.*, **95**, 855 (2022).
18. S. Daneshyan, G. Sodeifian, *J. Supercrit. Fluids*, **188**, 105679 (2022).
19. F. Hadizadeh, E. Khodaverdi, F. Oroojalian, P. Rahmanian-Devin, S. H. M. Hashemi, N. Omidkhah, K. Asare-Addo, A. Nokhodchi, H. Kamali, *Int. J. Pharm.*, **631**, 122507 (2023).
20. J. Shi, X. Kang, L. Mao, Y. Jiang, S. Zhao, Y. Liu, B. Zhai, H. Jin, L. Guo, *Chem. Eng. J.*, 141608 (2023).
21. L. Jia, L. Xu, Y. Liu, J. Hao, X. Wang, *CCS Chem.*, **5**, 510 (2023).
22. Á. Miguel, N. García, V. Gregorio, A. López-Cudero, P. Tiemblo, *Polymers*, **12**, 1336 (2020).
23. L. M. Sanchez, D. G. Actis, J. S. Gonzalez, P. M. Zélis, V. A. Alvarez, *J. Nanopart. Res.*, **21**, 1 (2019).
24. H. M. Nizam El-Din, A. W. M. El-Naggar, *Des. Monomers Polym.*, **17**, 322(2014).
25. D. Das, P. Prakash, P. K. Rout, S. Bhaladhare, *Starch-Stärke*, **73**, 1900284 (2021).
26. J. W. Tay, D. H. Choe, A. Mulchandani, M. K. Rust, *J. Econ. Entomol.*, **113**, 2061 (2020).
27. B. Tomadoni, C. Casalongué, V. A. Alvarez, *Poly. Agri-Food Appl.*, 99 (2019).
28. E. T. Tenório-Neto, T. Jamshaid, M. Eissa, M. H. Kunita, N. Zine, G. Agusti, H. Fessi, A. E. El-Salhi, A. Elaissari, *Polym. Adv. Technol.*, **26**, 1199 (2015).
29. M. R. Rahman, S. Hamdan, J. L. C. Hui, in: MATEC web of conferences, vol. 87, EDP Sciences. 2017, p. 03013.
30. M. S. H. Akash, K. Rehman, M. S. H. Akash, K. Rehman, *Ess. Pharma. Anal.*, 207 (2020).
31. R. R. F. Ramos, D. D. Siqueira, R. M. R. Wellen, I. F. Leite, G. M. Glenn, E. S. Medeiros, *J. Polym. Environ.*, **27**, 1677 (2019).
32. H. Gul, A. U. H. A. Shah, S. Gul, J. Arjomandi, S. Bilal, *Iran. J. Chem. Chem. Eng.*, **37**, 193 (2018).
33. A. S. Kipcak, F. T. Senberber, E. Moroydor Derun, N. Tugrul, S. Piskin, *Res. Chem. Intermed.*, **41**, 9129 (2015).
34. V. Rani, R. C. Srivastava, H. M. Agarwal, M. G. H. Zaidi, *Mat. Today: Proceed.*, **4** (9), 9471 (2017).
35. S. Mehtab, M. G. H. Zaidi, N. Rana, K. Khati, S. Sharma, *Bull. Mat. Sci.*, **45**, 162 (2022).